17

Light Intensity Fluctuations and Blueshift

Moon Kyu Choi
Hongik University
South Korea

1. Introduction

Chaos-like properties such as noise or fluctuations arising from quantum effects have recently investigated on a single barrier potential and on a one-dimensional periodic potential barrier. They used either the plane wave of light or a wavepacket (pulse) passing through the potential barrier, demonstrating the chaos created by the bounded one-dimensional multibarrier potential (Bar and Horwitz, 2002; Hondou and Sawada, 1995), and proved it is an ordered and periodic phenomenon. Also another group demonstrated unexpected behavior of a dissipative particle in simple multiscale systems subject to chaotic noise and clarified the reason for the particular behavior because it is under a periodic potential (Chialvo et al., 1997). They concluded the occurrence of drift in a symmetric periodic potential would be expected to be a common feature of noise-driven systems. Essentially this effect is quite similar to the problem of a particle placed in a potential well of finite barrier (Cohen-Tannoudji et al., 1977) and the present issue of the photon distribution on a crystallite surface.

When the crystallite size decreases to a few nanometers, the light absorption or photoluminescence in air moves to the direction of smaller wavelength, which is known as the blueshift (Kale and Lokhande, 2000; Nanda et al., 1999; Tsunekawa et al., 2003; Von Behren et al., 2000). The basic theory for this phenomenon is the quantum confinement effect (Andersen et al., 2002; Sharma et al., 2005). According to this theory the number of photons confined in each unit cell increases with the decreasing crystallite size. It is also said to enlarge the band gap between the valence band and the conduction band. Another approach is to take crystalline unit cells as numerical elements and employ different potential energies over a unit cell (Choi, 2007; Choi and Kim, 2007), realizing light intensity fluctuations. The effect of the film thickness on the blueshift was investigated by one of the authors (Choi and Pyun, 2008) about cellular crystalline surfaces with periodic potential, getting the blueshift numerically demonstrated in good agreement with experiments.

In this paper we deal with surface nanostructures and try to prove the blueshift numerically by predicting the location of absorption wavelength. One of the best ways to uphold the present numerical method would be to demonstrate the blueshift phenomenon observed widely experimentally (Lu et al., 2008; Miyake et al., 1999; Tan et al., 2005; Tsunekawa et al., 2000). They demonstrated experimentally the dependence of the blueshift on the crystallite size for CeO and CdS. One of the authors has been studying this problem recently, publishing a few papers (Choi, 2007; Choi and Kim, 2007; Choi and Pyun, 2008), and this paper may be taken as an extension of these consecutive efforts. Another publication (Choi and Choi, 2009) predicting the blueshift with respect to the shell layer thickness has been already accomplished and led the present investigation to be made.

Another possible and not-yet-practiced application from the same technique would be coating a heat radiant or absorbing surface with paint of nanoparticle dispersion. To save energy it is extremely important to have the best emissive or absorptive coefficient of radiation. It is desirable to find the criteria to produce such surfaces with a double layer having nanoparticles dispersed. The average distance between the nanoparticles is one of the important parameters that have a big influence on the emission or absorption. The present technique would be an excellent approach to that problem.

2. Theoretical background

We are considering a single-layer microsphere irradiated by monochromatic unpolarized light wave and investigate the realization of light intensity fluctuations at the absorption wavelengths. Figure 1 displays a schematic of the present situation. We want to show numerically the blueshift phenomenon observed experimentally. This is the phenomenon that the absorption (or the luminescence) wavelength decreases with decreasing unit cell or particle sizes (Andersen et al., 2002; Kale and Lokhande, 2000; Nanda et al., 1999; Sharma et al., 2005; Tsunekawa et al., 2003; Von Behren et al., 2000). Since this investigation is an extension of the former ones, most mathematical formulations are omitted here and only essential contents are stated. The details may be referred to in the previous publications (Choi, 2007; Choi and Kim, 2007; Choi and Pyun, 2008). Readers are especially advised that they see Ref. (Choi, 2001) for the modeling details. The electric and magnetic vectors in both the internal and the external regions must satisfy the macroscopic Maxwell equations that govern the behavior of electromagnetic fields. Taking the harmonic time dependence to be $\exp(-\imath\omega t)$ for all fields and assuming no free charge, we reduce the Maxwell equations to a set of vector wave equations for the electric field $\mathbf{E}$ and the magnetic field $\mathbf{H}$:

$$\bigtriangledown^2 \mathbf{E} + k^2 \mathbf{E} = 0, \tag{1}$$

$$\bigtriangledown^2 \mathbf{H} + k^2 \mathbf{H} = 0, \tag{2}$$

where k is the wave number, k = $\omega(\epsilon\mu)^{1/2}$, ϵ is the complex permittivity, and μ is the permeability.

It is very difficult to solve Eqs. (1) and (2) numerically. There are three scalar equations coupled to solve simultaneously for each layer, since Eqs. (1) and (2) are separate vector equations. To treat the present case, one has to solve nine equations in general simultaneously. One can derive, however, the governing equations for the Debye potentials, which are equivalent to Scrödinger equations, to represent the TM and TE modes from Eqs. (1) and (2) as done in the Mie method of solution. For the particle or the air outside the particle, the Debye potentials are governed by

$$\bigtriangledown^2 u + k^2 u = 0, \tag{3}$$

Note that the scalar governing equations for each layer are separate and independent of each other; this is the great advantage of employing the Debye potentials over solving Eqs. (1) and (2) directly.

One has to note that these transformed equations are, as a matter of fact, Schrödinger equations which govern the quantum behavior of particles, or photons in this case. The wave number, k, is related to the refractive index of particle or medium, N as follows.

$$k = \frac{N\omega}{c} \tag{4}$$

Here the frequency, ω, and the light speed in vacuum, c, are constant, but the refractive index changes depending on particle material. We know from the quantum mechanics that the wave number is also related to the potential energy (U) as

$$k^2 = (\mathrm{E} - \mathrm{U})\frac{8\pi^2 m}{h^2} \tag{5}$$

The significance of bigger wave number or higher refractive index is lower potential energy. In this study we want to treat a single-layer microsphere with crystalline unit cells covered on, so photons should experience different potential energies depending on whether they are placed on the edges of the cells or their inside. Figure 2 shows a typical graph of potential energies in the whole system, which is as similar a situation as finite well potentials in series. For a single photon particle making a harmonic oscillation in a particular coordinate let the displacement from the position of equilibrium be q (Denbigh, 1981). The potential energy is given by

$$U = \frac{1}{2}bq^2 \tag{6}$$

We need to separate the potential energy into two different regions, the edge and the inside of a unit cell. The edge value of the potential energy leads us to use a specific refractive index on the end points of numerical elements in order to solve Eq. (3). On the other hand, the inside quadratic variation of the potential energy may be approximated by taking linear averages of the endpoint values instead of solving Eq. (3). This approximating method saves us from finding the refractive index of the inside. If the size of a unit cell (or a crystallite) decreases, we may have a different value of b in Eq. (6), but here in this research we just make an *ad hoc* assumption that the value of b remains constant. Then with a new smaller unit cell we should have a smaller potential energy on the edge of the cell and thus the refractive index gets bigger (See Fig. 3).

The boundary element method developed recently by the author in a previous investigation (Choi, 2007) is extended to study an absorption problem on a single-layer sphere and suggest a method to predict the light intensities on a TiO_2 microsphere. Since the governing equations in the present investigation, the Helmholtz type equations, admit of the boundary-element formulation, one need only calculate two integral equations simultaneously for each surface. Since we are dealing with a single-layer microsphere here, we need to make two layers in a coated microsphere the same material.

There are many factors that influence light intensity fluctuations. Some of them are the crystalline size, the shell layer (or film) thickness, the particle size, etc. Besides other chemical and physical properties including chemical compositions, passivation and surface morphology may also be in effect. These implicit properties are represented by the refractive index (or the potential energy). We need to demonstrate blueshift theoretically somehow with one of those causes. The effect of the shell thickness on the blueshift was investigated in a previous research (Choi and Choi, 2009) and the blueshift was proved by the numerical approach. In this paper we especially want to study on the effects of the crystalline size on the blueshift, fixing other parameters. The realization of the blueshift by the boundary element method would be another great proof of the author's recent successive publications.

The properties of any thermodynamic system in macroscopic equilibrium with its surroundings, for instance, the energy, the density, etc., undergo microscopic fluctuations, but give us only average values. The intrinsic fluctuations in matter-density are most easily observed by the scattering of light which they produce in transparent systems. Another well-known example is the critical opalescence with the substance at the critical

point. The fluctuation-dissipation theorem (Chandler, 1987) expresses a relation between the susceptibility of an irreversible response and equilibrium fluctuations. Phenomenologically it is found that the flow of energy in a thermally conducting body is proportional to the gradient of the temperature. Likewise the electric potential difference causes the flow of electrons in a conductor. The phenomenological thermal and electrical conductivities are related to the autocorrelations of fluctuations of some properties. Similarly the energy conversion from one type to another may occur from the fluctuations of energy on the interface. This research area is named as fluctuation-induced transport (Chialvo et al., 1997).
The problem dealt with in the present investigation is about steady-state photon densities inside a microscale single-layer dielectric sphere, given the surface intensities of the incident light. The sphere may be, therefore, considered as a thermodynamic equilibrium system and the fluctuations of light intensities should be related to some kind of energy conversion rates by the fluctuation-dissipation theorem. The electron transfer among microstates can happen after a part of input photon energy is transferred to the particle surface. These excited electrons may contribute to photovoltaic effects, photocatalytic behaviors, and photoluminescence.

3. Results and discussion

We studied three cell (i.e., crystallite) sizes in the present investigation. Intuitively if the cell sizes reduce, the potential energy difference between the edges of a unit cell and its inside will be changed according to the Eq. (6). If we assume the parameter, b, in Eq. (6) remains constant over different crystallite sizes, then we can see that the refractive index on the edge of the smaller crystallite becomes larger. We will show, therefore, the numerical results obtained by increasing the refractive index (or decreasing potential energies) with decreasing cell size.
One of the main purposes of this paper is to demonstrate the blueshift numerically. For this purpose Table I and the following set of parameters are employed for typical demonstrations:

- light: 100 – 1100 nm wavelength at 10 nm intervals and unpolarized
- microparticle radius: 500 nm
- microsphere material: TiO_2
- medium outside the microsphere: air
- incident direction of light: +z-axis

Case	#1	#2	#3
cell size [nm]	3.00	2.52	2.17
refractive index of TiO_2	2.43+i0.01	2.83+i0.01	3.23+i0.01

Table 1. Parameters for modeling.

The numerical results obtained using these data are shown in Fig. 4–7. The angle in the x-axis of graphs is the azimuthal angle measured from the +z-axis, the light propagation direction as shown in Fig. 1. The value of +1 implies the peripheral location where the sphere is exposed to the incident light whereas -1 is the opposite location. The source functions are the ratio of the electric field magnitude of the incident light to that of the absorption light. One may regard this source function as the intensity ratio. Figures 4(a)–(d) display the source functions numerically calculated on the particle surface of crystallite size 3.0 nm. Parts (a) and (b) display surface intensity results at the interval of about 100 nm. As a matter of fact

calculations were done with the interval of 10 nm from 100 nm to 1100 nm in wavelength, but only representative results are shown. As one can see from part (b), fluctuations are remarkable at the wavelength of 700 nm and more detailed data from around it are shown in parts (c) and (d). One can observe fluctuations to occur notably between 680 nm and 720 nm. One may anticipate this wavelength will be the absorption peak when the absorption spectra are taken. If you look at the plots in part (b), you will find a little fluctuations with the wavelengths over 1000 nm. This happens because the ratio of the cell size to the wavelength is small enough in this region of wavelength (Choi and Kim, 2007). Thus we can expect there should be light absorption here too, and it is not related to jumping the bandgap, but to heat dissipation. Moreover, this latter region of wavelength yielding fluctuations is not our concern here because it is infrared (IR).

Then we had the crystallite size reduced to 2.51 nm by increasing the number of numerical elements on the particle surface. When one has two different crystallite sizes, the smaller crystallite may have a higher potential energy on the edge of the crystallite than the bigger one. Therefore, we need to increase the refractive index from the value (or 2.43 + i 0.01) which corresponds to the case of 3.0 nm crystallite size. The numerical results from the increased refractive index (or 2.83 + i 0.01) are shown in Fig. 5 (a)–(d) and we can see from part (b) that there are fluctuations around 620 nm (i.e., implying the blueshift), which are more in detail displayed in parts (c) and (d). We can see noticeable fluctuations over 800 nm, but it is as similar a phenomenon as observed in Fig. 4(b) at the wavelengths over 1000 nm with 3.00 nm crystallite size, and they are beyond our wavelength region of concern . Besides since the ratio of crystallite size to wavelength became lower here than in the former case, the incipient wavelength causing heat dissipation to move from 1000 nm to 800 nm.

We decreased the crystallite size further to 2.16 nm by increasing the number of numerical elements. As is the case with the crystallite size of 2.51 nm, the refractive index on the edge of unit cell is increased a little more to be 3.23+i0.01. The numerical results from this case are displayed in Fig. 6 (a)–(d). We can clearly see that the location of fluctuations moved to about 570 nm.

The above results of absorption wavelength are summarized in Fig. 7. The solid points are the representative absorption wavelengths yielding the strongest intensity fluctuations while the vertical line segments denote the ranges of wavelength where intensity fluctuations are seen. These representative wavelengths are thought to be the location where light is absorbed and it is, in other words, the bandgap. As was explained in the Introduction, the blueshift has been observed as the crystallite sizes reduce in semiconductor nanomaterials (Kale and Lokhande, 2000). According to the fluctuations-dissipation theorem, one can expect that light absorption happens at the wavelength showing fluctuations. Therefore, we could demonstrate the blueshift numerically by employing three crystallite sizes.

Figure 8 is the comparison of the present numerical results with the experiments (Von Behren et al., 2000) from another research group. This group was arbitrarily chosen since their data were available to be shown for comparison. A few other experimental results from other groups mentioned in the Introduction are in qualitative agreement with our numerical demonstration, but they did not display their results specifically and quantitatively enough to be presented here. Significant agreement can be seen in Fig.8 although the two results came from totally different situations of materials (i.e., refractive indices) and morphology.

4. Conclusion

A single-layer TiO_2 microsphere where the refractive index of microsphere is adjusted depending on the crystallite size is irradiated by monochromatic unpolarized light. We

could find the wavelength location where light absorption is highly probable because of severe intensity fluctuations. This wavelength location moves toward smaller wavelength (i.e., blueshift) as the crystallite size reduces. Qualitatively, this demonstration agrees with experiments from other research groups.

5. Acknowlegments

This work was supported by the 2010 Hongik University Academic Research Support Fund.

List of Figures

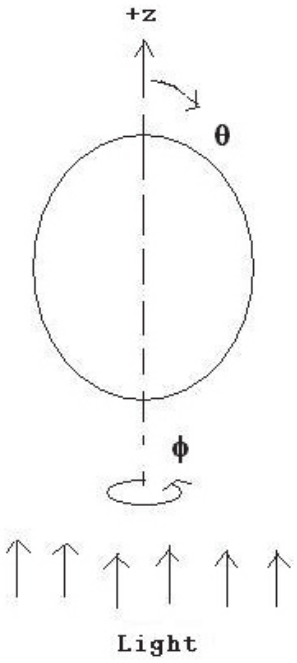

Fig. 1. Schematic diagram of a microsphere. The monochromatic unpolarized light irradiates a single-layer microsphere in the +z direction.

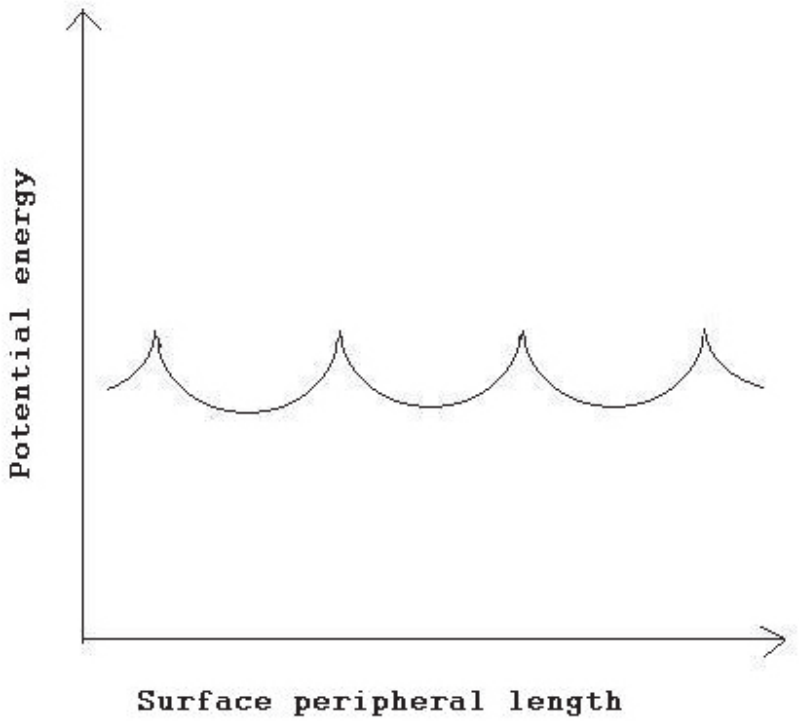

Fig. 2. The potential energy variation along a particle peripheral surface.

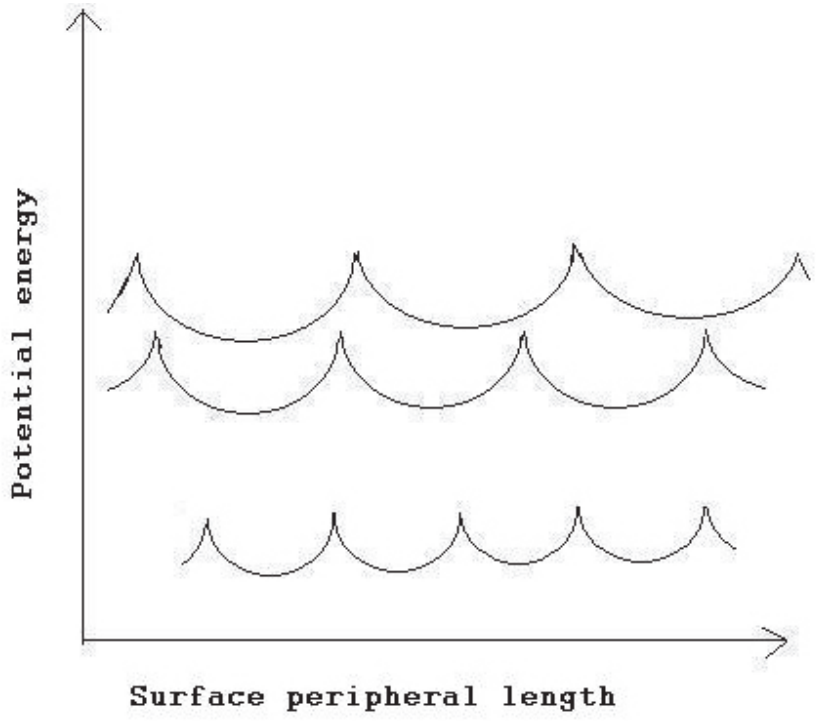

Fig. 3. The potential energy variation with the crystallite size reduction.

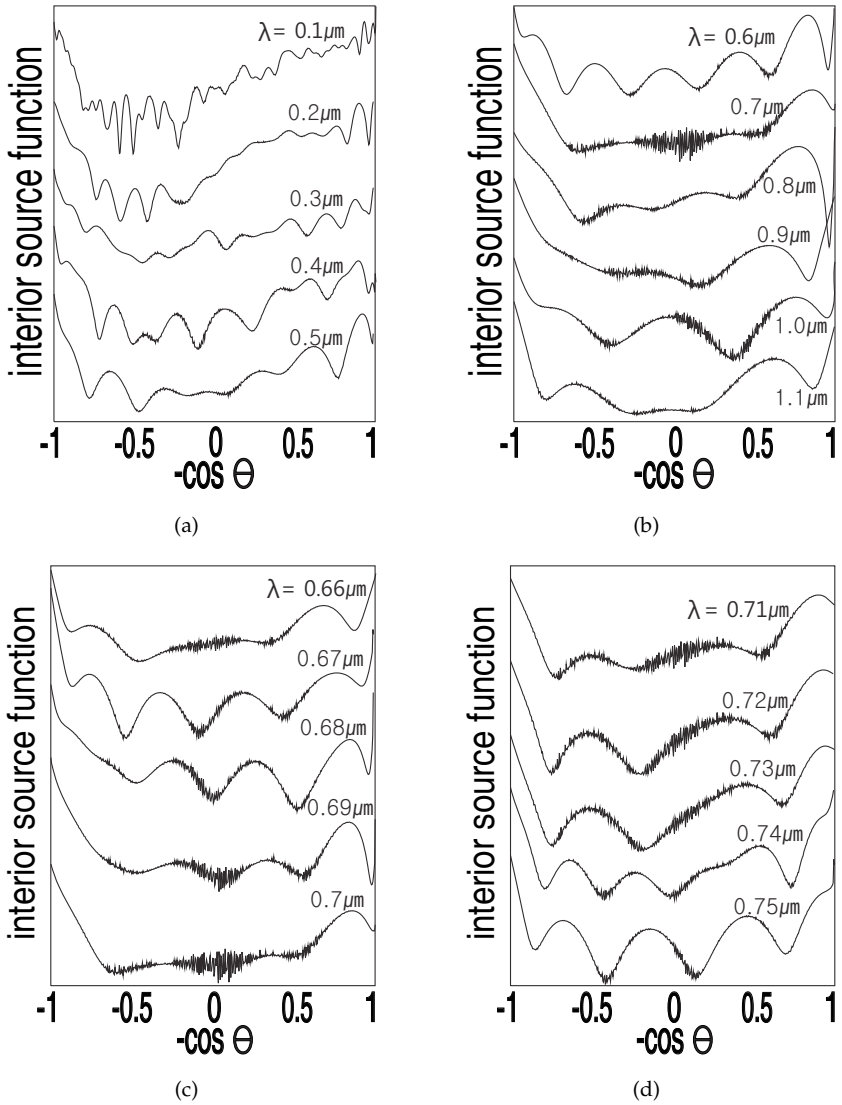

Fig. 4. Source functions vs. cos(angle) for a single-layer microsphere of 500 nm radius, the crystal size of 3.0 nm, and many different wavelengths. (a) For the wavelengths from 100 nm to 600 nm. (b) For the wavelengths from 700 nm to 900 nm. (c) and (d) More detailed data for wavelengths between 710 nm and 800 nm. The number of surface peripheral elements were 525. The refractive index on the unit cell edge was chosen to be 2.43+i0.01. The abscissa tic -1 corresponds to a point on the particle surface opposite the incident light (in the forward scattering direction) and +1 corresponds to the point nearest the incident light source (in the back scattering direction).

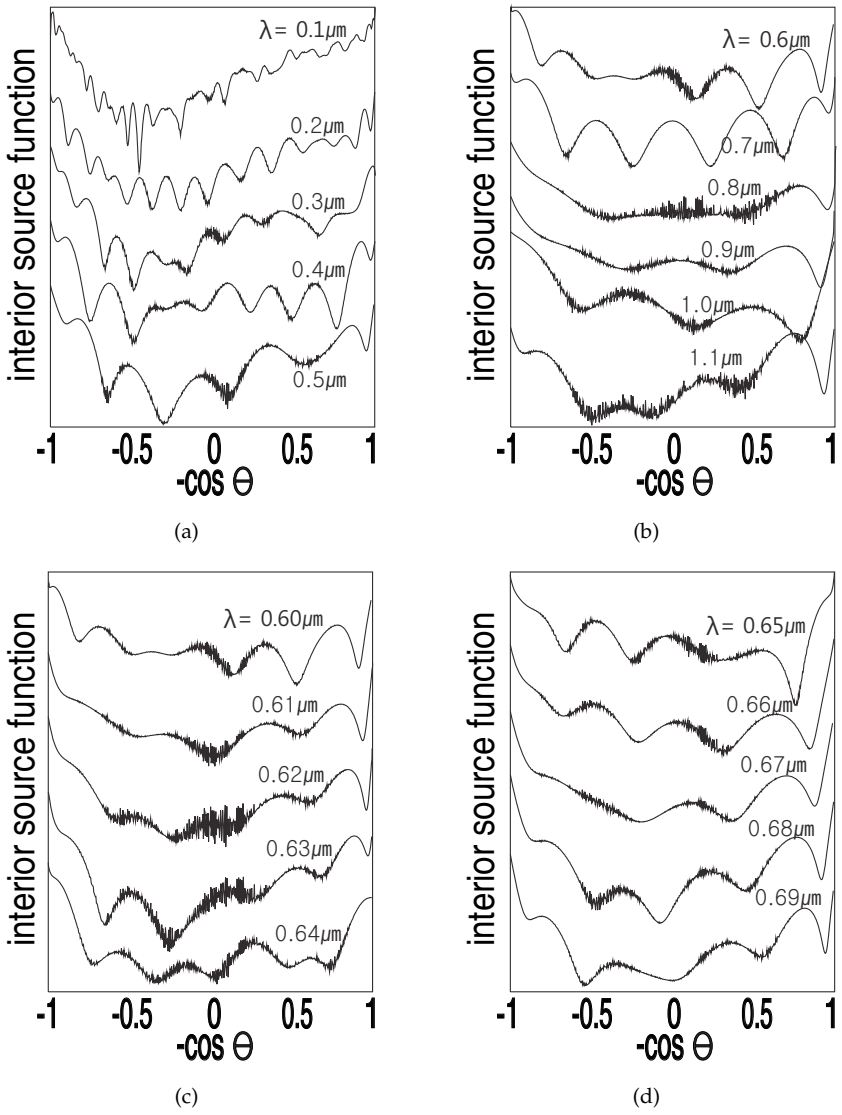

Fig. 5. Source functions vs. cos(angle) for a single-layer microsphere of 500 nm radius, the crystal size of 2.52 nm, and many different wavelengths. (a) For the wavelengths from 100 nm to 500 nm. (b) For the wavelengths from 600 nm to 1100 nm. (c) and (d) More detailed data for wavelengths between 600 nm and 690 nm. The number of surface peripheral elements were 625. The refractive index on the unit cell edge was chosen to be 2.83+i0.01.

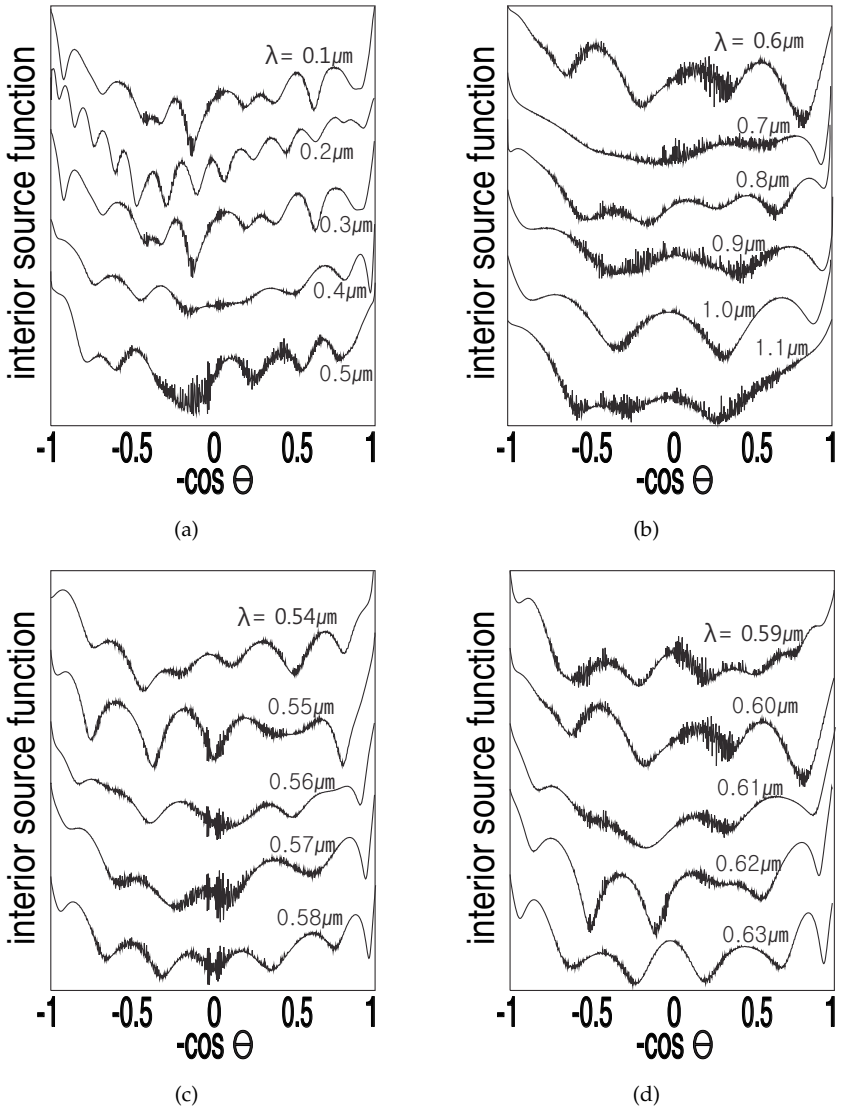

Fig. 6. Source functions vs. cos(angle) for a single-layer microsphere of 500 nm radius, the crystal size of 2.17 nm, and many different wavelengths. (a) For the wavelengths from 100 nm to 500 nm. (b) For the wavelengths from 600 nm to 1100 nm. (c) and (d) More detailed data for wavelengths between 540 nm and 630 nm. The number of surface peripheral elements were 725. The refractive index on the unit cell edge was chosen to be 3.23+i0.01.

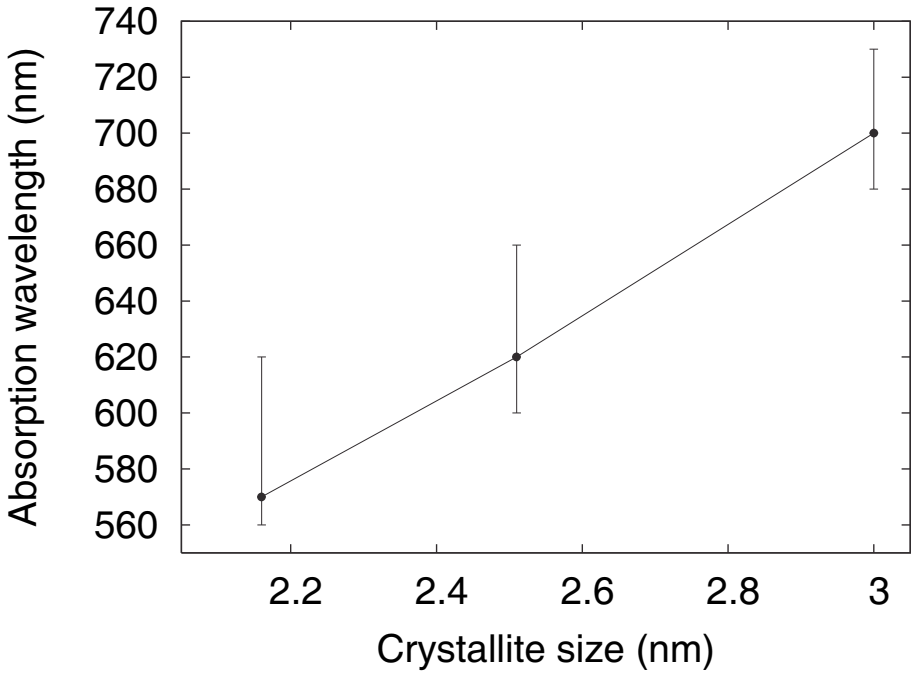

Fig. 7. The absorption wavelengths versus the crystallite sizes are summarized here after their identifications from Figs. 4–6. The points are the exact locations of wavelength for the strongest fluctuations while the vertical bars represent a range where fluctuations are seen.

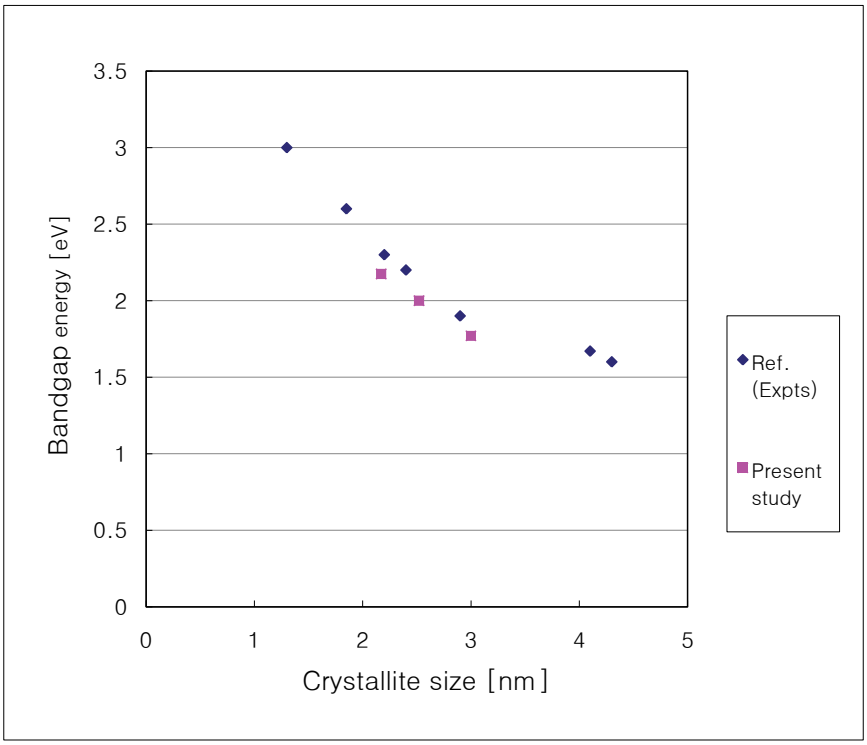

Fig. 8. The bandgap energies and the blueshift from the present numerical demonstrations are displayed together with experimental results reproduced from Ref. (Von Behren et al., 2000).

6. References

Andersen, K. E.; Fong, C. Y. & Pickett, W. E. (2002). Quantum confinement in CdSe nanocrystallites. *J. Non-Cryst. Solids*, Vol. 299-302, 1105–1110.

Bar, D. & Horwitz, L. P. (2002). Dynamical effects of a one-dimensional multibarrier potential of finite range. *Eur. Phys. J. B*, Vol. 25, 505–518.

Chandler, D. (1987). *Introduction to Modern Statistical Mechanics*, Oxford University Press, New York.

Chialvo, D. R.; Dykman, M. I. & Millonas, M. M. (1997). Fluctuation-induced transport in a periodic potential: noise versus chaos. *Phys. Rev. Lett.*, Vol. 78, No. 8, 1605.

Choi, M. K. (2001). Numerical calculation of light scattering from a layered sphere by the boundary-element method. *J. Opt. Soc. Am. A*, Vol. 18, 577–583.

Choi, M. K. (2007). Light intensity fluctuations on a layered microsphere irradiated by a monochromatic light wave: Modeling of an inhomogeneous cellular surface with numerical elements. *Mater. Sci. Eng. B*, Vol. 137, 138–143.

Choi, M. K. & Choi, Y. (2009). Numerical demonstration of the blueshift of the light absorption wavelength for a layered microsphere: Effects of shell thickness on the blueshift. *J. Korean Phys. Soc.*, Vol. 54, No. 6, 2309–2317.

Choi, M. K. & Kim, J. (2007). Light intensity fluctuations on a semiconductor microsphere calculated by boundary element method. *Curr. Appl. Phys.*, Vol. 7, 622–628.

Choi, M. K. & Pyun, J. (2008). Light intensity and its fluctuations on a layered microsphere: Effects of shell thickness acting as a quantum well. *Curr. Appl. Phys.*, Vol. 8, 603–611.

Cohen-Tannoudji, C.; Diu, B. & Lalo, F. ë (1977). *Quantum Mechanics*, Wiley, New York.

Denbigh, K. (1981). *The Prnciples of Chemical Equilibrium*, Cambridge University Press, Cambridge.

Hondou, T. & Sawada, Y. (1995). Dynamical Behavior of a Dissipative Particle in a Periodic Potential Subject to Chaotic Noise: Retrieval of Chaotic Determinism with Broken Parity. *Phys. Rev. Lett.*, Vol. 75, No. 18, 3269–3272.

Kale, S. S. & Lokhande, C. D. (2000). Thickness-dependent properties of chemically deposited CdSe thin flims. *Mater. Chem. and Phys.*, Vol. 62, No. 2, 103–108.

Lu, S. G., Mak; C. L., Pang; G. K. H.; Wong, K. H. & Cheah, K. W. (2008). Blue-shift and intensity enhancement of photoluminescence in lead-zirconate-titanate-doped silica nanocomposites. *Nanotechnology*, Vol. 19, 1–4.

Miyake, M.; Torimoto, T.; Sakata, T.; Mori, H. & Yoneyama, H. (1999). Photoelectrochemical characterization of nearly monodisperse CdS nanoparticles-immobilized gold electrodes. *Langmuir*, Vol. 15, 1503–1507.

Nanda, K. K.; Sarangi, S. N. & Sahu, S. N. (1999). Visible light emission from CdS nanocrystals. *J. Phys. D: Appl. Phys.*, Vol. 32, 2306–2310.

Sharma, S. N.; Kohli, S. & Rastogi, A. C. (2005). Quantum confinement effects of CdTe nanocrystals sequestered in TiO2 matrix: effect of oxygen incorporation. *Physica E*, Vol. 25, 554–561.

Tan, S. T.; Chen, B. J.; Sun, X. W.; Fan, W. J.; Kwok, H. S.; Zhang, X. H. & Chua, S. J. (2005). Blueshift of optical bandgap in ZnO thin films grown by metal-organic chemical-vapor deposition. *J. Appl. Phys.*, Vol. 98, 013505.

Tsunekawa, S.; Fukuda, T. & Kasuya, A. (2000). Blue shift in ultraviolet absorption spectra of monodisperse $CeO_{2?x}$ nanoparticles. *J. Appl. Phys.*, Vol. 87, 1318–1321.

Tsunekawa, S.; Wang, J.-T.; Kawazoe, Y. & Kasuya, A. (2003). Blueshifts in the ultraviolet absorption spectra of cerium oxide nanocrystallites.*J. Appl. Phys.*, Vol. 94, 3654–3656.

Von Behren, J.; Wolkin-Vakrat, M.; Jorne, J. & Fauchet, P. M. (2000). Correlation of photoluminescence and bandgap energies with nanocrystal sizes in porous silicon. *J. Porous Materials*, Vol. 7, 81–84.

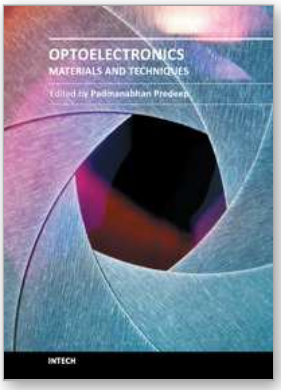

Optoelectronics - Materials and Techniques

Edited by Prof. P. Predeep

ISBN 978-953-307-276-0
Hard cover, 484 pages
Publisher InTech
Published online 26, September, 2011
Published in print edition September, 2011

Optoelectronics - Materials and Techniques is the first part of an edited anthology on the multifaceted areas of optoelectronics by a selected group of authors including promising novices to the experts in the field. Photonics and optoelectronics are making an impact multiple times the semiconductor revolution made on the quality of our life. In telecommunication, entertainment devices, computational techniques, clean energy harvesting, medical instrumentation, materials and device characterization and scores of other areas of R&D the science of optics and electronics get coupled by fine technology advances to make incredibly large strides. The technology of light has advanced to a stage where disciplines sans boundaries are finding it indispensable. Smart materials and devices are fast emerging and being tested and applications developed in an unimaginable pace and speed. Here has been made an attempt to capture some of the materials and techniques and underlying physical and technical phenomena that make such developments possible through some real time players in the field contributing their work and this is sure to make this collection of essays extremely useful to students and other stake holders such as researchers and materials scientists in the area of optoelectronics.

How to reference

In order to correctly reference this scholarly work, feel free to copy and paste the following:

Moon Kyu Choi (2011). Light Intensity Fluctuations and Blueshift, Optoelectronics - Materials and Techniques, Prof. P. Predeep (Ed.), ISBN: 978-953-307-276-0, InTech, Available from: http://www.intechopen.com/books/optoelectronics-materials-and-techniques/light-intensity-fluctuations-and-blueshift

INTECH
open science | open minds

InTech Europe
University Campus STeP Ri
Slavka Krautzeka 83/A
51000 Rijeka, Croatia
Phone: +385 (51) 770 447
Fax: +385 (51) 686 166
www.intechopen.com

InTech China
Unit 405, Office Block, Hotel Equatorial Shanghai
No.65, Yan An Road (West), Shanghai, 200040, China
中国上海市延安西路65号上海国际贵都大饭店办公楼405单元
Phone: +86-21-62489820
Fax: +86-21-62489821